



Low- $\delta^{18}\text{O}$ mantle-derived magma in Panjal Traps overprinted by hydrothermal alteration and Himalayan UHP metamorphism: Revealed by SIMS zircon analysis

Hafiz Ur Rehman ^{a,*}, Kouki Kitajima ^b, John W. Valley ^b, Sun-Lin Chung ^{c,d}, Hao-Yang Lee ^{c,d}, Hiroshi Yamamoto ^a, Tahseenullah Khan ^e

^a Graduate School of Science and Engineering, Kagoshima University, Kagoshima 890-0065, Japan

^b WiscSIMS Laboratory, Department of Geoscience, University of Wisconsin, 1215 W. Dayton St., Madison, WI 53706, USA

^c Department of Geosciences, National Taiwan University, Taipei, Taiwan

^d Institute of Earth Sciences, Academia Sinica, Taipei, Taiwan

^e Department of Earth and Environmental Sciences, Bahria University, Islamabad, Pakistan

ARTICLE INFO

Article history:

Received 13 July 2017

Received in revised form 1 November 2017

Accepted 3 December 2017

Available online 28 December 2017

Handling Editor: A.S. Collins

Keywords:

Himalaya

Kaghan

Eclogites

Panjal Traps

In situ SIMS $\delta^{18}\text{O}$ analysis

Zircon oxygen isotopes

ABSTRACT

We report two generations of low- $\delta^{18}\text{O}$ zircons from the Himalayan eclogites and their host gneisses. In situ SIMS $\delta^{18}\text{O}$ analyses on single zircon crystals (with known age and Hf isotope ratios) from two populations of chemically distinct zircons demonstrate a complex history: (1) an early low- $\delta^{18}\text{O}$ mantle-derived magma, (2) followed by post-emplacement high-temperature meteoric-water alteration and finally (3) crystallization of new, low- $\delta^{18}\text{O}$ minerals during the ultrahigh-pressure metamorphism. Magmatic zircon (269 Ma) in Group I eclogites yielded $\delta^{18}\text{O}$ values from 1.9 to 4.6‰ VSMOW with an average value of 4.0 ± 0.2 (n = 35, the error is 2SD analytical precision and “n” represents number of analyzed spots), which is lower than the typical mantle values (5.3 ± 0.6 , 2SD). In contrast, metamorphic zircons (45 Ma) in Group II eclogites preserve unusually low, negative $\delta^{18}\text{O}$ values from -3.9 to -2.7 ‰ (average: -3.4 ± 0.4 , n = 35, 2SD). Zircons in felsic gneiss that surround Group II eclogites have inherited magmatic cores (ca. 260 Ma) with $\delta^{18}\text{O}$ values of ca. 2.9‰, which decrease to -0.1 ‰ in metamorphic (ca. 45 Ma) rims. These zircons preserve lower $\delta^{18}\text{O}$ values than would be equilibrated with typical mantle. The low- $\delta^{18}\text{O}$ values in magmatic zircons suggest that the mafic protolith to these eclogites formed from a hydrothermally altered subducted oceanic crust and the negative $\delta^{18}\text{O}$ values in metamorphic zircons indicate hydrothermal alteration after crystallization of the mafic magmas but before growth of metamorphic zircons. This study reports evidence for melting of subducted low- $\delta^{18}\text{O}$ ocean crust to form low- $\delta^{18}\text{O}$ mantle-derived mafic magmas as previously proposed by Cartwright and Valley (1991, *Geology* 19, 578–581) for Proterozoic Scourie Dikes.

© 2017 International Association for Gondwana Research. Published by Elsevier B.V. All rights reserved.

1. Introduction

The $\delta^{18}\text{O}$ values (defined as $[(^{18}\text{O}/^{16}\text{O})_{\text{sample}} \div ^{18}\text{O}/^{16}\text{O}_{\text{STD}}] - 1] \times 1000$ in which the STD is Vienna Standard Mean Ocean Water; VSMOW) of mantle-derived magmas (basalts and gabbro) exhibit a narrow range of ca. $+5.7 \pm 0.3$ ‰ (Eiler, 2001; Valley et al., 2005; Hoefs, 2015). The fairly homogenous $\delta^{18}\text{O}$ composition of a majority of mantle-derived rocks results because most of the mantle is well mixed in $\delta^{18}\text{O}$ and the oxygen isotope composition during magmatic fractionation remains almost the same. However, eclogite facies mantle nodules and silicate inclusions in diamond attest to mantle domains of subducted ocean crust with anomalous values of $\delta^{18}\text{O}$ that have been

preserved (Garlick et al., 1971; Schulze et al., 2013). Higher $\delta^{18}\text{O}_{\text{Wole-rock}}$ values (>6 ‰) are interpreted as upper oceanic crust that was altered by low temperature interaction with seawater and low $\delta^{18}\text{O}$ values (-0 to 5 ‰) are attributed to high temperature alteration of lower oceanic crust. Melting tends to homogenize these extreme values, but rare low- $\delta^{18}\text{O}$ mantle-derived magmas have been identified that are proposed to result from melting of subducted lower oceanic crust (Cartwright and Valley, 1991, 1992; Wei et al., 2002; Davies et al., 2015).

Low- $\delta^{18}\text{O}$ values can form subsolidus in metamorphic rocks through high temperature hydrothermal alteration by surface (marine or meteoric) water (Valley, 1986; Criss and Taylor, 1986; Zheng et al., 2003). Understanding the timing and source of low $\delta^{18}\text{O}$ values is crucial. However, it is difficult to determine the original magmatic source of metamorphic rocks with mixed protolith and complex evolutionary histories. Oxygen isotope ratios, combined with U–Pb age, and multi-

* Corresponding author.

E-mail address: hafiz@sci.kagoshima-u.ac.jp (H.U. Rehman).

isotope geochemistry, provide significant information regarding the nature of the source magma from which the rocks have crystallized and how they have been geodynamically evolved through time.

Zircon is a common accessory mineral in igneous, sedimentary, and metamorphic rocks, which provides a robust tool to unravel the history of Earth's crust and mantle. Zircons have been widely studied for U–Pb age dating, Hf isotopes, trace element geochemistry, and oxygen isotope ratios. Because of its chemical and physical inertness and resistance to alteration, crystalline zircon (i.e., not radiation damaged) can retain compositions from crystallization (Wasserburg et al., 1969; Compston et al., 1984; Gebauer, 1996; Liati and Gebauer, 1999; Belousova et al., 2010; Valley, 2003; Valley et al., 2005, 2015; Liu et al., 2006). Moreover, due to the extremely slow diffusion rate of oxygen in zircon (Watson and Cherniak, 1997; Zheng and Fu, 1998; Peck et al., 2003; Page et al., 2007; Bowman et al., 2011) it can preserve the original $\delta^{18}\text{O}$ values of the source from which it crystallized. Thus, zircons can provide the key for understanding the evolutionary history of rocks. If zircons are zoned or have chemically distinct domains (Chen et al., 2011), then combined in situ U–Pb age, Hf isotope, and $\delta^{18}\text{O}$ data in zircon provide critical information to trace back the geodynamic evolution from magmatic to post-magmatic, and subsequent metamorphic events.

In this study we report very low and negative $\delta^{18}\text{O}$ values of magmatic and metamorphic zircons (with known U–Pb age and Hf isotope compositions; Rehman et al., 2013a, 2016) from Himalayan eclogites and their host gneisses. The aim of this study is to determine the composition of pre-eclogite magmas from which these rocks formed and how they hydrothermally altered. Finally, what happened to their chemistry when these rocks were subjected to ultrahigh-pressure metamorphism at mantle depths (coesite-stability) and subsequent exhumation. These results yield significant insight into the evolution of the Indian plate before and after its breakup from Gondwana and the Eocene India-Asia collision.

2. Sample description and geological background

In this study six 25-mm diameter zircon mounts were analyzed: two mounts from one sample of high-pressure (HP) Group I eclogite (Ph380_Zrn2 and Ph380_Zrn3); two mounts containing zircons from three samples (Ph422, Ph423, and Ph425) of ultrahigh-pressure (UHP) Group II eclogites (“A” and “B”); and two mounts of zircons from two UHP felsic gneisses that surround the Group II eclogites (Ph416 and Ph427). Petrological details of Groups I and II eclogites and felsic gneisses were discussed elsewhere (Rehman et al., 2014, 2016, 2017). A brief description of the samples used in this study is presented below.

Both groups of eclogite and felsic gneiss were collected from the Higher Himalayan crystalline sequence in the Kaghan Valley, Pakistan (Fig. 1). Group I eclogites are medium to coarse-grained, composed of garnet porphyroblasts, omphacite, amphibole, and symplectites replacing garnet and omphacite with abundant rutile, titanite, and ilmenite. Zircons are abundant and relatively large (~500 μm). Pressure-temperature conditions of 2.2 ± 0.3 GPa and 704 ± 92 °C were previously reported from this group (Rehman et al., 2013b). Group II eclogites are composed of garnet, omphacite, phengite, epidote, and quartz/coesite, with accessory rutile, titanite and a few small zircons (<200 μm). Group II eclogites recorded conditions around 2.7–3.2 GPa and 727–786 °C confirming their UHP stability (O'Brien et al., 2001; Kaneko et al., 2003; Rehman et al., 2007). Felsic gneisses are composed of quartz, white mica, biotite, plagioclase and epidote with accessory rutile, titanite, apatite, allanite and zircon. Felsic gneisses do not preserve UHP phases in the matrix or as inclusions in major porphyroblasts however coesite inclusions in zircons from felsic gneiss (Rehman et al., 2016) confirm their UHP history. The protolith of both types of eclogite (as well as other low-grade metabasites) were proposed to be derived from large-scale magmatic activity (known as the Panjal Traps) on the Indian plate in the Permian (for details see Rehman et al., 2016, and references therein). The relatively coarser grained Group I eclogites were

probably derived from gabbroic protolith whereas the finer-grained Group II eclogites, preserving UHP phases, most likely developed from basaltic protolith. Mafic lithologies, older than Permian, are rare or have not been reported from the western Himalaya. However, granitic rocks of Cambro-Ordovician age (ca. 460 to 490 Ma) and associated mafic and felsic volcanics have been identified along the entire Himalayan range indicating an extensive regional orogenic event in the northern Indian continent (e.g. Mansehra granite in Pakistan, Mandi granite in India, Bhimphedian granite in Nepal, and bimodal volcanism in southwest Yunnan and Tibet in China) which were interpreted to represent the northern margin of east Gondwana (Miller et al., 2001; Cawood et al., 2007; Zhu et al., 2012; Naeem et al., 2016).

3. Analytical techniques

Most of the zircons of this study were previously analyzed for U–Pb and Hf isotopes (see Rehman et al., 2016). In this study, in situ analysis of oxygen isotope ratios ($^{18}\text{O}/^{16}\text{O}$) was performed on zircon grains using a CAMECA IMS 1280 ion microprobe at the WiscSIMS Laboratory of the University of Wisconsin-Madison, following established procedures (Kita et al., 2009; Valley and Kita, 2009; Kitajima et al., 2012). Oxygen isotopes were analyzed using a 2.0–2.2 nA primary $^{133}\text{Cs}^+$ beam with ~10 μm spot size. Secondary ^{16}O and ^{18}O ions were measured simultaneously using two Faraday cup detectors. As a monitor of “water” and radiation damage, $^{16}\text{O}^1\text{H}$ was analyzed simultaneously with ^{18}O and ^{16}O and from the same pit (Wang et al., 2014). On all six 25-mm diameter mounts, chips of KIM-5 zircon (WiscSIMS standard with $\delta^{18}\text{O} = 5.09\%$ VSMOW, Valley, 2003) were mounted at the center and sample zircon grains were within 7 mm of the center. All the mounts were re-polished to keep the standard and other grains at equal height. Topography of the sample surface was checked by profilometer before analysis to ensure all the grains are at the same height as surrounding epoxy. Zircon mounts were ultrasonically cleaned with deionized water and alcohol, and gold coated prior the SIMS analysis. Oxygen isotope data were acquired for all six mounts in a single 12-hour session. The average value of eight standard analyses bracketing each group of 10 to 14 analyses of unknowns was used for instrumental mass bias correction. The precision of individual analyses is estimated by two standard deviations (2SD) of the reproducibility of bracketing standard analyses and measured values for this session average <0.3‰ (Valley and Kita, 2009). The results of $^{18}\text{O}/^{16}\text{O}$ ratios are reported in per mil “‰” notation relative to the Vienna Standard Mean Ocean Water (VSMOW).

4. Results

A total of 97 spots (two to three spots on each of 43 zircon grains) on six mounts were measured for $\delta^{18}\text{O}$. Measured spots on Groups I and II eclogite, and felsic gneisses are shown in Figs. 2, 3, 4, respectively. Near the measured spots, we also show U–Pb age and $\varepsilon\text{Hf}(t)$ values for previously analyzed grains (from Rehman et al., 2016). Data for the analyzed zircons are shown in Table 1, and the data with all details for the analyzed zircons and standards are provided in Supplementary Table S1 (available on line). Values of $\delta^{18}\text{O}$ range from 1.9 to 4.6‰ (average = 4.0 ± 0.2 standard's external error here and elsewhere when stated, $n = 35$ in which notation “n” means number of analyzed spots) in zircons of Group I eclogites, from -3.8 to -2.7% (average: -3.4 ± 0.4 , $n = 35$) in zircons of Group II eclogites, and from -0.1 to 2.9‰ (average: 1.1 ± 0.1 , $n = 27$) in zircons of felsic gneiss. The $\delta^{18}\text{O}$ values of zircons in Group I eclogites are relatively variable but within a limited range. These values could be attributed to the earlier events and have been potentially acquired from the magmatic source. In contrast, $\delta^{18}\text{O}$ values of zircons in Group II eclogites display a narrow range from a more homogenized protolith (Fig. 5). The $\delta^{18}\text{O}$ values in two distinct populations of zircons are in accord with the U–Pb age data from the analyzed grains in which the former group yielded ages related to the magmatic events and the later produced ages representing the Himalayan UHP eclogite

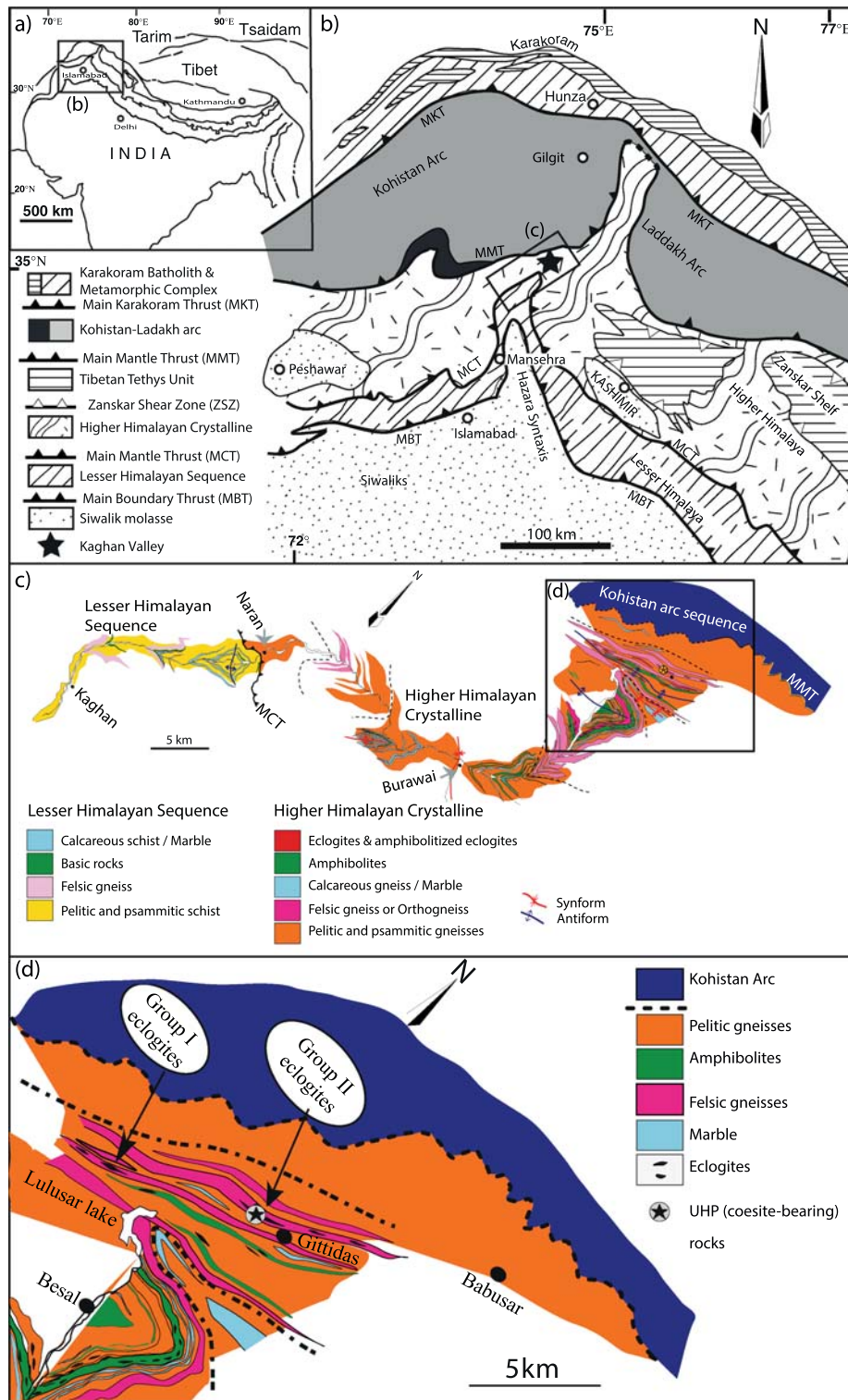


Fig. 1. Geological map of the study area (a) regional geological sketch, (b) major tectonic units of the western Himalaya, (c) geological cross-section along the Kaghan Valley transect with sample location, and (d) an enlarged view of a portion where the samples were collected.

facies event. There was no distinction for core vs. rim domains in Group I zircons and most of the dated spots show protolith-related ages (Fig. 2, also see Rehman et al., 2016). Several spots show younger ages than the geologically known events for the eclogite protolith; however they show no significant difference in $\delta^{18}\text{O}$ values. In contrast, all of the zircon grains in Group II eclogites are metamorphic in origin (containing inclusions of garnet, omphacite, and rutile) representing growth/recrystallization during the Himalayan UHP event (Fig. 3) and we could

distinguish core and rim domains in zircons from the felsic gneisses (seen via SEM-CL images) in which the core yielded ages identical or slightly younger than those obtained from the zircons of Group I eclogites and the rim yielded metamorphic ages coeval to those of zircons in Group II eclogites (Fig. 4). It is worthy of note that all the grains from both types of eclogite and from the surrounding felsic gneisses preserve $\delta^{18}\text{O}$ values lower than the typical mantle-equilibrated range (Fig. 6), however Group II eclogites show anomalously low, negative

$\delta^{18}\text{O}$ values. Zircons in felsic gneisses also exhibit lower $\delta^{18}\text{O}$ values and core domains preserve relatively higher $\delta^{18}\text{O}$ values compared with the rim or outer domains (Fig. 5).

5. Discussion

The $\delta^{18}\text{O}$ values in zircons (Group I, II, and felsic gneisses) exhibit a narrow range within each group and are significantly lower than those equilibrated with the mantle. Whole-rock and other constituent minerals from the three rock types also show lower than the typical mantle equilibrated values (zircon and whole rock data are shown in Fig. 7; other data are presented in Supplementary Table S2, reproduced from Rehman et al., 2014). These features suggest that one or more of the following scenarios account for the unusually low $\delta^{18}\text{O}$ values in the studied samples. First, hydrothermal alteration of the source of Panjal magmas occurred, prior to subduction, followed by low- $\delta^{18}\text{O}$ fluid (meteoric water) interaction at high temperature with the protolith of eclogites, then low $\delta^{18}\text{O}$ metamorphic minerals were formed during high-temperature metamorphism from their precursors. In the forthcoming sections we discuss these scenarios in detail. The narrow range of $\delta^{18}\text{O}$, U–Pb age concordance and low OH/O ratios indicate that the studied zircons preserve primary mineral compositions

and thus rule out a fourth possibility; the analyzed $\delta^{18}\text{O}_{\text{zircon}}$ values were not affected by secondary alteration or radiation damage.

Crystalline, non-metamict zircon, due to its resistance to hydrothermal alteration (Valley et al., 1994, 2005; Watson and Cherniak, 1997; Zheng and Fu, 1998; Wei et al., 2002; Zheng et al., 2004), preserves $\delta^{18}\text{O}$ of the magma from which it crystallized. However, under higher temperatures (>800 to 900 °C) the values of $\delta^{18}\text{O}$ in crystalline zircon may partially reset due to diffusion (e.g. Valley, 2003; Page et al., 2007; Bowman et al., 2011). In contrast, zircons with high levels of radiation damage, domains within zircon become amorphous (metamict) and are easily altered. There are many tests that, in combination, permit identification of such non-crystalline material, including: discordance of U–Pb ages, CL zoning patterns, magnetism, solubility in HF, trace element compositions, low birefringence, microcracks and OH/O ratios (Valley, 2003; Wang et al., 2014; Valley et al., 2005, 2015). We carefully investigated the analyzed zircons in this study to determine if they incorporate any significantly damaged domains or metamictization. Most of the analyzed spots in zircons of Group I eclogite yielded U–Pb ages (ca. 259 ± 10 Ma) that plot on Concordia.

The positive $\epsilon\text{Hf}(t)$ values cluster around +10 (ranging between +4.2 and +14.5) represent a juvenile mantle source with almost no crustal component (see Rehman et al., 2016 for details on Hf isotope discussion). Zircons in Group II eclogite are more homogeneous in

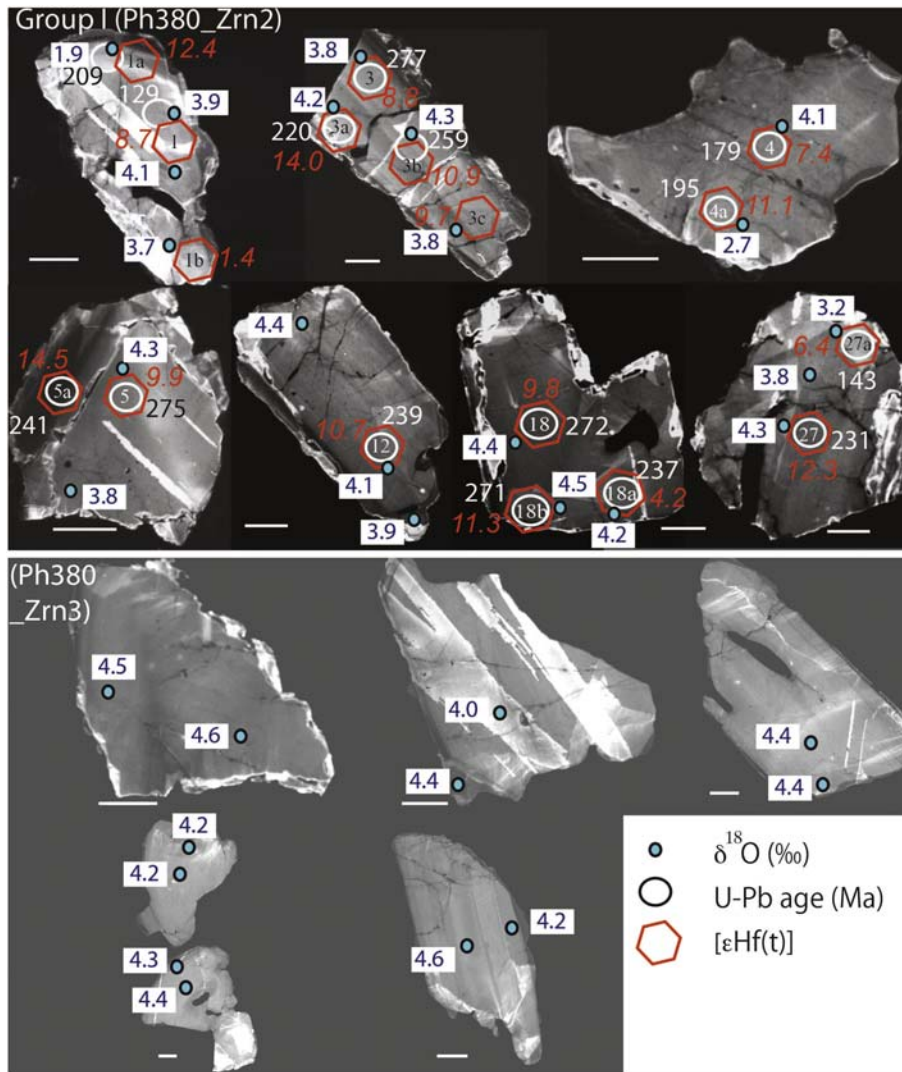
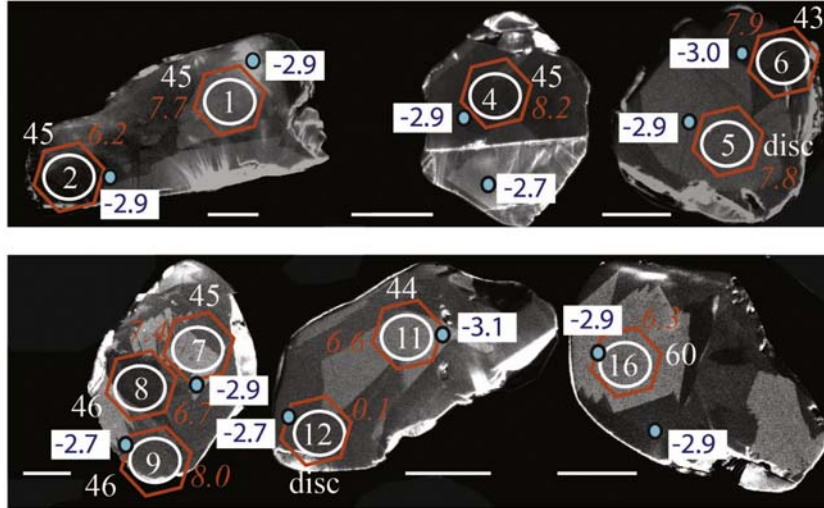


Fig. 2. SEM-cathodoluminescence images of the analyzed zircons from Group I eclogites. Numbers in the circles with a, b, c suffixes are the zircon numbers (to see them in Table S1). The same grains were analyzed for LA-ICP-MS U–Pb and Hf isotope ratios. In situ SIMS $\delta^{18}\text{O}$ analyses are also shown. Zircons from mount Ph380_Zrn3 were picked from same sample (Ph380) and were analyzed for $\delta^{18}\text{O}$ values only. We assume those grains have identical age and Hf isotope composition. Scale bar shown for each grain is 50 μm .

Group II zircons (Mount A)



Group II zircons (Mount B)

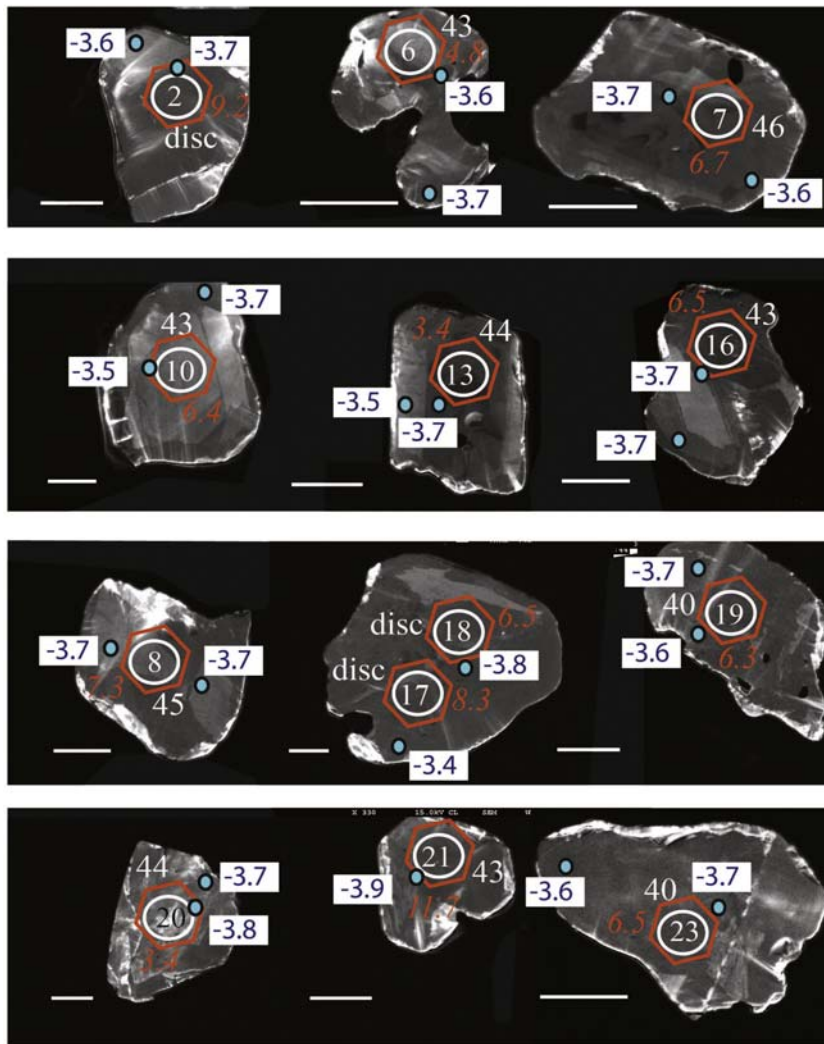


Fig. 3. SEM-cathodoluminescence images of the analyzed zircons from Group II eclogites. Other details are the same as in Fig. 2; disc. = discordant in age.

geochemical features showing U–Pb ages within a narrow range (41 to 53 Ma, average: 48 ± 3 , 1SD) also plot on Concordia. The $\epsilon_{\text{Hf}}(t)$ values in this group cluster around +7 (ranging between +3.4 to +8.9) and

represent a common juvenile mantle source similar to that of Group I zircons. These features suggest that Group I zircons represent magmatic crystallization at ~269 Ma while Group II formed from the

Felsic gneiss (Ph427)

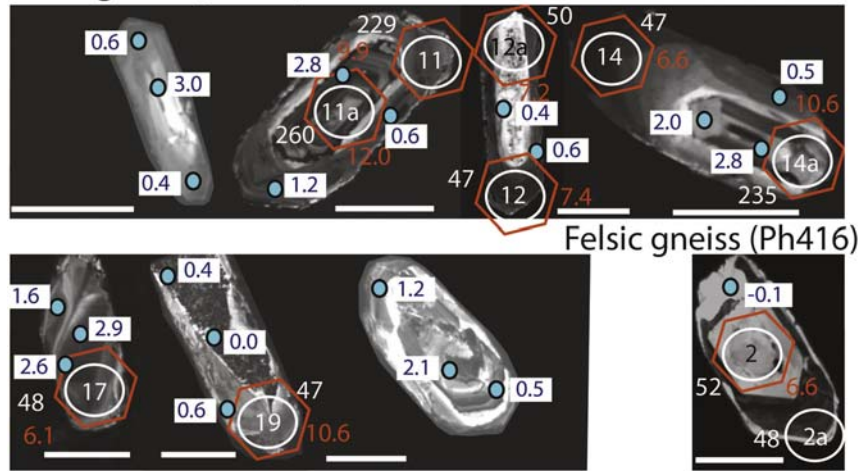


Fig. 4. SEM-cathodoluminescence images of the analyzed zircons from felsic gneisses. Other details are the same as in Fig. 2.

crystallization of new zircons during metamorphism of hydrothermally altered low- $\delta^{18}\text{O}$ rocks (Fig. 7). We also took care not to analyze areas close to the healed cracks or above visible micro inclusions. Our data show extremely low background-corrected $^{16}\text{O}^1\text{H}/^{16}\text{O}$ ratios (Supplementary Table S1) and there is no correlation of $^{16}\text{O}^1\text{H}/^{16}\text{O}$ versus $\delta^{18}\text{O}$ (Fig. 8). This evidence further attests that no secondary alteration was experienced by those zircons; hence the oxygen isotope data reported here are unaltered and geologically meaningful.

Moreover, solid-state diffusive exchange of oxygen can be observed with obvious steep gradients under the extreme temperature conditions (e.g. ultrahigh-temperature metamorphism $>800^\circ\text{C}$: Page et al., 2007; Bowman et al., 2011). The studied samples have experienced HP to UHP eclogite facies metamorphism (750–800 $^\circ\text{C}$). Diffusive exchange, even if it occurred, should be relatively slower at such conditions. Therefore, the protolith-related U–Pb age in magmatic zircons in Group I eclogite as well as the core domains of zircons in felsic gneisses most likely preserve the parent magma $\delta^{18}\text{O}$ values whereas the newly grown metamorphic zircons in Group II eclogite have likely acquired unusually low $\delta^{18}\text{O}$ values from metamorphic growth in lower $\delta^{18}\text{O}$ rocks. In contrast, Group II zircons and rim domains in zircons from felsic gneisses likely grew under UHP conditions at 750–800 $^\circ\text{C}$ and hence record metamorphic equilibration of isotope ratios and trace element compositions. The negative $\delta^{18}\text{O}$ values of zircons in Group II eclogites record the composition of the whole rock prior to metamorphism. That is why $\delta^{18}\text{O}$ values in garnet and omphacite are nearly identical to those of zircons. However, magmatic zircons in Group I eclogites retain $\delta^{18}\text{O}$ values from their parent magma. During later exhumation stages, the $\delta^{18}\text{O}_{\text{zircon}}$ values were unchanged because of the relatively slower diffusion rate of oxygen in crystalline zircon.

The $\delta^{18}\text{O}$ values in UHP felsic gneisses are also low compared to normal granitic, volcanic or metasedimentary rocks (Fig. 6). Zircons in felsic gneisses retain low but slightly positive $\delta^{18}\text{O}$ values in core domains, but have negative values in rim domains. These features indicate two episodes of high temperature hydrothermal alteration. The protolith of felsic magmas was altered by low- $\delta^{18}\text{O}$ water before melting and the igneous rocks exchanged with heated meteoric water after solidification, which further reduced $\delta^{18}\text{O}$ to negative values. Finally, the hydrothermally altered, low- $\delta^{18}\text{O}$ protoliths were transformed into eclogites and gneisses when these rocks reached mantle depths (>90 km; coesite stability) in the Eocene during the India-Asia collision. Values of $\delta^{18}\text{O}$ equilibrated among the metamorphic mineral assemblages under the HP/UHP conditions. During late exhumation, fluids from the surrounding metasedimentary rocks (carbonates/pelites) potentially once again modified $\delta^{18}\text{O}$ values of some minerals to be equal or higher than the typical mantle range, as can be seen in the amphibolites ($\delta^{18}\text{O}_{\text{whole-rock}}$

$\sim 5.8\text{‰}$) and greenschist ($\delta^{18}\text{O}_{\text{whole-rock}} \sim 9.2\text{‰}$, Supplementary Table S2, reproduced from Rehman et al., 2014).

A correlation of $\delta^{18}\text{O}$ between quartz and zircon, if seen with appropriate fractionation ($\delta^{18}\text{O}_{\text{quartz-zircon}} \sim 2\text{‰}$ at magmatic temperatures, Valley et al., 2003), would suggest that both minerals were isotopically equilibrated at higher temperatures when zircon crystallized. However, in the $\delta^{18}\text{O}_{\text{quartz}}$ versus $\delta^{18}\text{O}_{\text{zircon}}$ plot (Fig. 9), the $\delta^{18}\text{O}_{\text{quartz-zircon}}$ data from Group I plot away from the quartz-zircon ($\Delta^{18}\text{O}_{\text{quartz-zircon}} = 2\text{‰}$) equilibration line (please note that the data plotted represent an average value of all the analyzed spots). These features indicate that metamorphism or any other secondary events did not modify the zircon oxygen isotope data from the time of its magmatic crystallization. To further confirm that the $\delta^{18}\text{O}_{\text{zircon}}$ is primary, we plot $\delta^{18}\text{O}_{\text{garnet}}$ versus $\delta^{18}\text{O}_{\text{zircon}}$ in the same figure (Fig. 9) in which garnet-zircon data in Group I also plot away from the garnet-zircon equilibration line ($\Delta^{18}\text{O}_{\text{garnet-zircon}} = 0\text{‰}$). This evidence supports our interpretation that $\delta^{18}\text{O}_{\text{zircon}}$ is primary and did not equilibrate with $\delta^{18}\text{O}_{\text{garnet}}$. For the Group II where all zircons are metamorphic, the $\delta^{18}\text{O}_{\text{quartz-zircon}}$ data plot further away from the quartz-zircon equilibration line, indicating that the $\delta^{18}\text{O}$ values of zircon and quartz were not in equilibrium during metamorphism. In contrast, $\delta^{18}\text{O}_{\text{garnet}}$ versus $\delta^{18}\text{O}_{\text{zircon}}$ in Group II plot along and parallel to the garnet-zircon equilibration line, indicating that garnet and metamorphic zircons in Group II eclogites acquired lower, nearly identical $\delta^{18}\text{O}$ values when they were in equilibrium during eclogite facies metamorphism ($\Delta_{\text{garnet-zircon}} \sim 0.1\text{‰}$ for almandine-pyropite at metamorphic temperatures, Valley, 2003). These metamorphic minerals acquired the low- $\delta^{18}\text{O}$ values from the metamorphic protolith. In contrast, zircons in Group I eclogites preserve higher $\delta^{18}\text{O}$ values than those found in garnet in the same group, indicating lack of equilibration among igneous zircons and eclogite facies minerals.

5.1. Low- $\delta^{18}\text{O}$ mafic magma

Rehman et al., 2014 discussed the possibility of a low- $\delta^{18}\text{O}$ magma reservoir for the Permian Panjal Traps based on bulk analysis of $\delta^{18}\text{O}$ in whole-rock powders and minerals. In this study, based on the new in situ $\delta^{18}\text{O}$ data from magmatic and metamorphic zircons from the same rocks, we present further insights for magma genesis and post-magmatic evolution.

There are numerous examples of low- $\delta^{18}\text{O}$ magmas that formed in the crust, including: Icelandic basalts (Hartley et al., 2013), felsic volcanics from Yellowstone and other centers of the Snake River Plain (Bindeman and Valley, 2001; Bindeman et al., 2008; Blum et al., 2016), UHP eclogites and granitic gneisses from the Dabie-Sulu orogenic belt in eastern China (Zheng et al., 1998; Rumble et al., 2002; Wei et al.,

Table 1
Oxygen isotope data for the zircon from the Himalayan UHP rocks measured by CAMECA IMS 1280 at WiscSIMS.

Analysis#	Sample	$\delta^{18}\text{O}$ ‰ VSMOW	2SD (ext.)	$\delta^{18}\text{O}$ ‰ measured	2SE (int.)
Group I (Ph380_Zrn2)					
88	Zrn18_1	4.39	0.23	4.73	0.20
89	Zrn18_2	4.49	0.23	4.84	0.21
90	Zrn18_3	4.23	0.23	4.58	0.23
91	Zrn01_1	1.95	0.23	2.29	0.16
92	Zrn01_2	3.92	0.23	4.26	0.16
93	Zrn01_3	4.09	0.23	4.44	0.21
94	Zrn01_4	3.67	0.23	4.01	0.20
95	Zrn03_1	3.83	0.23	4.17	0.22
96	Zrn03_2	4.18	0.23	4.52	0.22
97	Zrn03_3	4.32	0.23	4.67	0.26
98	Zrn03_4	3.79	0.23	4.13	0.23
103	Zrn04_1	4.09	0.22	4.31	0.17
104	Zrn04_2	2.71	0.22	2.93	0.17
105	Zrn05_1	4.33	0.22	4.54	0.22
106	Zrn05_2	3.81	0.22	4.02	0.20
107	Zrn08_1	3.67	0.22	3.89	0.14
108	Zrn08_2	3.74	0.22	3.95	0.24
109	Zrn12_1	4.07	0.22	4.28	0.24
110	Zrn12_2	3.87	0.22	4.08	0.24
111	Zrn12_3	4.45	0.22	4.66	0.20
112	Zrn24_1	4.57	0.22	4.78	0.17
113	Zrn24_2	4.48	0.22	4.70	0.25
114	Zrn27_1	3.18	0.22	3.39	0.15
115	Zrn27_2	3.78	0.22	4.00	0.23
116	Zrn27_3	4.33	0.22	4.55	0.21
Group I (Ph380_Zrn3)					
169	Zrn20_1	4.43	0.22	4.64	0.18
170	Zrn20_2	4.40	0.22	4.61	0.22
171	Zrn21_1	4.16	0.22	4.37	0.19
172	Zrn21_2	4.17	0.22	4.38	0.20
173	Zrn22_1	4.43	0.22	4.64	0.19
174	Zrn22_2	4.34	0.22	4.55	0.24
175	Zrn19_1	4.05	0.22	4.26	0.17
176	Zrn19_2	4.39	0.22	4.60	0.24
177	Zrn23_1	4.62	0.22	4.83	0.24
178	Zrn23_2	4.19	0.22	4.40	0.21
Group II (Mount A)					
66	423_Zrn07_1	-2.89	0.63	-2.21	0.17
67	423_Zrn07_2	-2.87	0.63	-2.19	0.21
68	423_Zrn15_1	-2.91	0.63	-2.24	0.16
69	423_Zrn15_2	-2.68	0.63	-2.01	0.16
70	425_Zrn02_1	-2.95	0.63	-2.28	0.17
71	425_Zrn02_2	-3.04	0.63	-2.37	0.19
72	425_Zrn03_1	-2.91	0.63	-2.24	0.22
73	425_Zrn03_2	-2.69	0.63	-2.02	0.19
74	425_Zrn06_1	-3.12	0.63	-2.44	0.32
75	425_Zrn06_2	-2.75	0.63	-2.08	0.18
76	425_Zrn18_1	-2.87	0.63	-2.20	0.22
77	425_Zrn18_2	-2.90	0.63	-2.23	0.23
Group II (Mount B)					
28	422_Zrn01_1	-3.66	0.27	-2.23	0.23
29	422_Zrn01_2	-3.56	0.27	-2.13	0.23
30	422_Zrn02_1	-3.80	0.27	-2.37	0.15
31	422_Zrn02_2	-3.68	0.27	-2.26	0.14
32	422_Zrn05_1	-3.86	0.27	-2.43	0.20
33	422_Zrn07_1	-3.70	0.27	-2.27	0.21
34	422_Zrn07_2	-3.60	0.27	-2.17	0.21
35	423_Zrn18_1	-3.70	0.27	-2.27	0.18
36	423_Zrn18_2	-3.66	0.27	-2.23	0.19
37	423_Zrn23_1	-3.79	0.27	-2.36	0.32
38	423_Zrn23_2	-3.45	0.27	-2.03	0.21
44	425_Zrn03_1	-3.64	0.29	-2.17	0.20
45	425_Zrn03_2	-3.68	0.29	-2.21	0.19
46	425_Zrn04_1	-3.72	0.29	-2.26	0.20
47	425_Zrn04_2	-3.56	0.29	-2.09	0.22
48	425_Zrn05_1	-3.71	0.29	-2.24	0.24
49	425_Zrn05_2	-3.71	0.29	-2.24	0.18
50	425_Zrn07_1	-3.54	0.29	-2.07	0.21
51	425_Zrn07_2	-3.75	0.29	-2.28	0.23
52	425_Zrn11_1	-3.67	0.29	-2.20	0.22
53	425_Zrn11_2	-3.53	0.29	-2.07	0.24

Table 1 (continued)

Analysis#	Sample	$\delta^{18}\text{O}$ ‰ VSMOW	2SD (ext.)	$\delta^{18}\text{O}$ ‰ measured	2SE (int.)
54	425_Zrn17_1	-3.72	0.29	-2.25	0.22
55	425_Zrn17_2	-3.64	0.29	-2.17	0.20
Felsic gneiss (Ph427)					
125	Zrn3_1	0.87	0.09	1.29	0.30
126	Zrn3_2	1.06	0.09	1.49	0.17
127	Zrn3_3	0.90	0.09	1.32	0.23
128	Zrn4_1	0.13	0.09	0.55	0.19
129	Zrn4_2	0.45	0.09	0.87	0.26
130	Zrn4_3	0.79	0.09	1.21	0.21
131	Zrn11_1	2.85	0.09	3.27	0.19
132	Zrn11_2	0.64	0.09	1.06	0.22
133	Zrn11_3	1.19	0.09	1.61	0.20
134	Zrn10_1	3.04	0.09	3.46	0.14
135	Zrn10_2	0.57	0.09	0.99	0.23
136	Zrn10_3	0.42	0.09	0.84	0.23
141	Zrn12_1	0.36	0.12	0.77	0.21
142	Zrn12_2	0.61	0.12	1.01	0.17
143	Zrn14_1	2.85	0.12	3.26	0.23
144	Zrn14_2	0.51	0.12	0.92	0.21
145	Zrn14_3	1.97	0.12	2.38	0.22
146	Zrn17_1	2.60	0.12	3.01	0.20
147	Zrn17_2	1.63	0.12	2.04	0.19
148	Zrn17_3	2.86	0.12	3.27	0.18
149	Zrn19_1	0.65	0.12	1.06	0.22
150	Zrn19_2	0.00	0.12	0.41	0.25
151	Zrn20_1	2.07	0.12	2.47	0.14
152	Zrn20_2	0.47	0.12	0.87	0.19
153	Zrn20_3	1.23	0.12	1.63	0.17
154	Zrn19_3	0.45	0.12	0.85	0.17
Felsic gneiss (Ph416A)					
164	Zrn2_1	-0.09	0.11	0.21	0.21

The precision of individual analyses was estimated by two standard deviations (2SD) of the reproducibility of bracketing standard analyses.

2008; Fu et al., 2013; Wan et al., 2013; He et al., 2016) and mafic dykes of the Anorogenic Koegel Fontein Complex, South Africa (Curtis et al., 2013). Low $\delta^{18}\text{O}$ values in Icelandic basalts were due to the magmatic assimilation of altered low- $\delta^{18}\text{O}$ wallrocks during its ascent through the crust (Hartley et al., 2013). In mafic dykes of the Koegel Fontein Complex, the lower $\delta^{18}\text{O}$ values (ca. -2‰) were attributed to the

partial melting of hydrothermally altered low- $\delta^{18}\text{O}$ country rocks forming low $\delta^{18}\text{O}$ -depleted crustal magmas (Curtis et al., 2013).

Partial melting of hydrothermally altered volcanics was proposed by several authors for the genesis of low $\delta^{18}\text{O}$ rhyolites of the Snake River Plain (e.g. Bindeman and Valley, 2001; Blum et al., 2016). For eastern China eclogites, the low or negative $\delta^{18}\text{O}$ values were acquired by melting or assimilation of low- $\delta^{18}\text{O}$ crustal rocks (e.g. Yui et al., 1995; Wang et al., 2011; Fu et al., 2013; He et al., 2016 and references therein). Additionally, low $\delta^{18}\text{O}$ granite in northeast China was formed by the partial

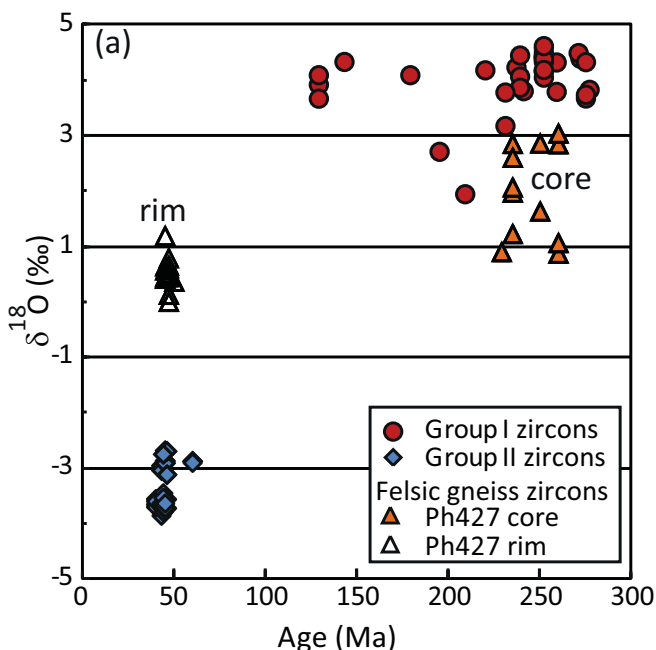


Fig. 5. SIMS $\delta^{18}\text{O}$ values in zircon plotted against U–Pb age (Ma).

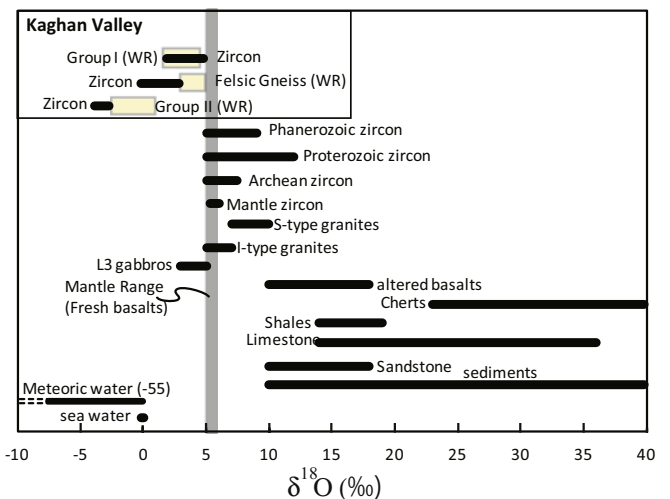


Fig. 6. Values of $\delta^{18}\text{O}$ in zircons (dark thick line) and whole rock (boxes) from eclogites and gneisses of the Kaghan Valley. Data for other rock types and for zircons of different origins are also shown for comparison. (Data adopted from Valley et al., 2005).

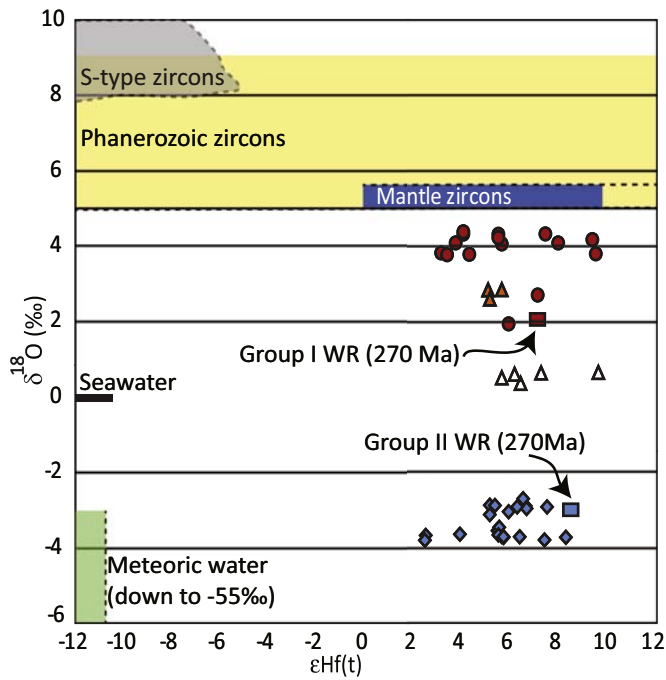


Fig. 7. Values of $\delta^{18}\text{O}$ for zircons and whole-rock (WR) plotted against $\epsilon\text{Hf}(t)$. Data for zircons of different origin are shown for comparison (data for $\delta^{18}\text{O}$ adopted from [Valley et al., 2005](#) and [Valley and Kita, 2009](#)). Symbols used are same as in [Fig. 5](#). Values for $\delta^{18}\text{O}$ of seawater and meteoric water are arbitrarily plotted along the Y-axis and do not imply a value of $[\epsilon\text{Hf}(t)]$.

melting of hydrothermally altered crustal material which exchanged with low- $\delta^{18}\text{O}$ surface fluids at high temperature during the continental rift tectonics associated with the breakup of Rodinia supercontinent ([Wei et al., 2002](#); [Zheng et al., 2007, 2008](#); [He et al., 2016](#)).

In contrast to crustal magmas, low- $\delta^{18}\text{O}$ magmas that formed in the mantle are rare. Low $\delta^{18}\text{O}$ tholeiitic magmas intruded the Lewisian Complex to form Scourie dikes in the Paleoproterozoic ([Cartwright and Valley, 1991, 1992](#); [Davies et al., 2015](#)). These magmas are interpreted to be uncontaminated and represent primitive mantle melts formed from melting of subducted oceanic crust that was hydrothermally altered before subduction ([Cartwright and Valley, 1991](#)). The low $\delta^{18}\text{O}$ values of zircons in Group I eclogites (average = 4.0‰) suggest melting of a low- $\delta^{18}\text{O}$ source. As the values of $\delta^{18}\text{O}$ in zircon of Group I eclogites are lower (1.9 to 4.6‰) than the mantle values (4.7 to 5.9‰) they reflect a source that was hydrothermally altered by surface waters (seawater or meteoric water) prior to magma generation.

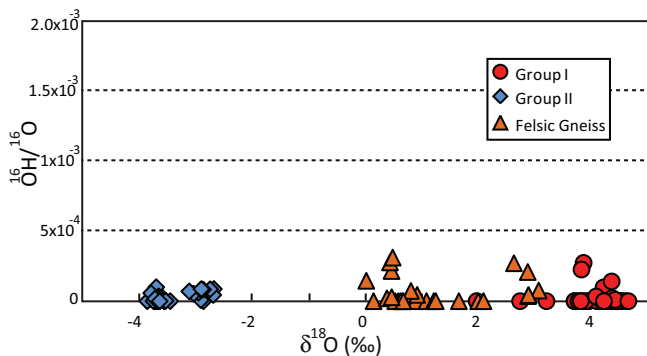


Fig. 8. Values of $\delta^{18}\text{O}$ plotted against background-corrected ratios of $^{16}\text{O}^1\text{H}/^{16}\text{O}$ (Supplementary Table S1). The concentration of water and OH is negligible in these zircons and there is no correlation with $\delta^{18}\text{O}$, indicating an absence of secondary effects or radiation damage.

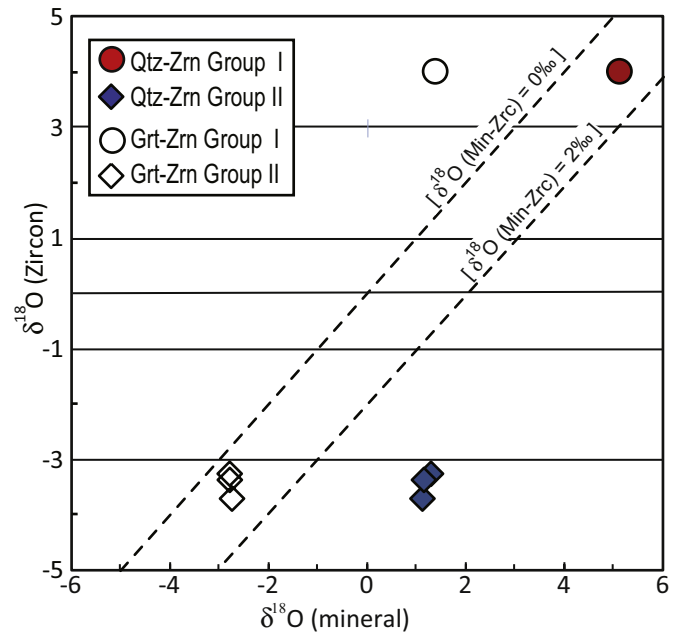


Fig. 9. Values of $\delta^{18}\text{O}$ for zircon (averaged for all the analyzed spots) plotted against averaged values of quartz and garnet for the samples from same group. The equilibration lines are drawn as $\delta^{18}\text{O}_{\text{quartz-zircon}} = 2\text{‰}$, and $\delta^{18}\text{O}_{\text{garnet-zircon}} = 0\text{‰}$. 2SD error bars are not shown as they are smaller than the symbol size plotted on the figure.

The negative $\delta^{18}\text{O}$ in Group II zircons (-3.9 to -2.7‰) and those in the whole rock cannot be formed without the meteoric water-rock interaction. To explain the process of seawater-hydrothermal alteration of the source, we have to look back at the tectonic scenario of the Indian plate-Tethyan-Asian subduction and collision. A significant component of the Tethyan oceanic crust, north of the MMT (suture between Indian plate and Kohistan-Ladakh Arc), has been subducted before the India-Asia collision. However there is no coherent oceanic crustal mass within the Himalayan metamorphic belt (except the Panjal mafic volcanics) south of MMT. In fact, crust forming events in Cambro-Ordovician time (ca. 460 to 490 Ma) along the northern margin of Indian continent during an Andean-type proto-Tethyan subduction (e.g. [Miller et al., 2001](#); [Cawood et al., 2007](#); [Zhu et al., 2012](#); [Naem et al., 2016](#)) may have played a significant role to underplate the oceanic crust and possibly contributed to the parent magma of the Permian Panjal Traps. Our hypothesis is consistent with the model of [Cawood et al. \(2007\)](#), see their [Fig. 5](#) who proposed that mafic underplating, terrane accretion, and crustal thickening occurred in the Cambro-Ordovician. We speculate that part of the hydrothermally altered subducted oceanic crust could have melted and formed the protolith of Himalayan eclogites during the Permian Panjal Trap extensive magmatism (continental flood basalts and feeder dikes).

Hafnium isotope data provide further insights on the origin of magmatic source. The Hf isotope data from the analyzed zircons in Groups I and II eclogites, and felsic gneiss show an average depleted mantle (T_{DM}) model age of 487 Ma (ranging from 307 to 709 Ma, $n = 20$) for Group I zircons, 455 Ma (ranging from 242 to 569 Ma, $n = 38$) for Group II zircons, and 440 Ma (ranging from 300 to 573 Ma, $n = 22$) for zircons in felsic gneiss (see [Table 3](#) in [Rehman et al., 2016](#)). The Hf model age does not represent the age of zircon crystallization but is the time at which the Hf of a crustal rock was isolated from its depleted mantle source. The Hf average T_{DM} model age from the studied zircons fits well with the magmatic source of Cambro-Ordovician orogenic events reported along the eastern margin of Gondwana. The 460 to 490 Ma Mansehra granite, located south of the Kaghan Valley ([Naem et al., 2016](#)), the 496 ± 14 Ma tholeiitic mafic rocks of Mandi pluton in India ([Miller et al., 2001](#)), the 475 Ma Bhimphedi granites in Nepal

(Cawood et al., 2007), and the bimodal volcanism in Tibet (Zhu et al., 2012) indicate asthenospheric upwelling and crustal extension tectonics during the Cambro-Ordovician time. All the zircons analyzed in this study yield positive $\epsilon_{\text{Hf}}(t)$ values indicating their source was segregated from a short-lived juvenile mantle crust. We suspect the low- $\delta^{18}\text{O}$ values in magmatic zircons (Group I) were acquired from the remelting of the hydrothermally altered subducted oceanic crust.

In contrast to values of $\delta^{18}\text{O}_{\text{zircon}}$ that are low, but positive, alteration by low- $\delta^{18}\text{O}$ meteoric water is necessary to form negative $\delta^{18}\text{O}$ values as preserved in the zircons of Group II eclogites, felsic gneisses, and those preserved in whole rock samples. This would require at least minimum initial water $\delta^{18}\text{O}$ values $< -8\%$ or even lower to produce negative $\delta^{18}\text{O}$ -bearing rocks. After the Panjal Trap magmatism the mafic and associated lithologies (including sedimentary successions) could have been severely altered by low- $\delta^{18}\text{O}$ meteoric water, which lowered $\delta^{18}\text{O}$ values of the exchangeable minerals in the whole-rock, but did not exchange with refractory minerals like zircon (Supplementary Table S2, available on line). Values of $\delta^{18}\text{O}$ in Group II eclogites (whole rock and most of the constituent minerals, excluding late-stage phases) are much lower than in Group I (Rehman et al., 2014). Rocks with such negative $\delta^{18}\text{O}$ values cannot be produced without meteoric water interaction at high temperatures. None of the ages analyzed in zircons from Group II eclogites are reasonable magmatic ages for the protolith. The evidence clearly demonstrates that the metamorphic domains (ca. 45 Ma) acquired $\delta^{18}\text{O}$ values from their pre-metamorphic precursors. The rim domains of zircons in felsic gneisses (ca. 45 Ma) also preserve low- $\delta^{18}\text{O}$ values and further support our interpretation that the post-magmatic protoliths of both types of rocks (mafic and felsic) were hydrothermally altered by meteoric water before subduction-related metamorphism.

5.2. Post-magmatic meteoric water-rock interaction

As discussed earlier, seawater-rock interaction ($\delta^{18}\text{O}_{\text{sea water}} = 0\%$) will not form negative $\delta^{18}\text{O}$ values in rocks even at high temperature ($> 300\text{ }^\circ\text{C}$). Likewise, meteoric water of -4% at low near-surface temperatures ($< 100\text{ }^\circ\text{C}$) cannot alter basaltic rocks (5.7%) to negative $\delta^{18}\text{O}$ values even if the water-rock interaction ratios are high (see Zhao and Zheng, 2003). Altering mantle-composition rocks to values of $\delta^{18}\text{O}$ below -3% will require involvement of meteoric water. These lines of evidence show that heated meteoric water-rock interaction likely altered the Panjal basaltic rocks after crystallization and these low or negative $\delta^{18}\text{O}_{\text{whole-rock}}$ values were preserved despite UHP metamorphism during the India-Asia collision-related subduction. The $\delta^{18}\text{O}$ of zircons in both groups of low- $\delta^{18}\text{O}$ eclogite confirm seawater hydrothermal alteration of the pre-magmatic source, followed by post-magmatic meteoric water hydrothermal alteration. Magmatic core domains of zircons in felsic gneisses (with U–Pb ages of 260 Ma) show a trend of decrease in $\delta^{18}\text{O}_{\text{zircon}}$ values ca. 2.9 to -0.1% from the magmatic cores towards metamorphic rims. Prolonged meteoric water-rock interaction can be traced from the negative $\delta^{18}\text{O}_{\text{whole-rock}}$ values, but zircons, once crystallized (e.g., Group I), will faithfully preserve the $\delta^{18}\text{O}$ value from its parent magma. Thus, metamorphic zircons in Group II eclogites and rim domains of zircons in felsic gneisses acquired low- $\delta^{18}\text{O}$ values from later conditions when they grew. This interpretation is supported by $\delta^{18}\text{O}_{\text{whole-rock}}$ values that are significantly lower than $\delta^{18}\text{O}_{\text{zircon}}$ in Group I eclogites indicating post-magmatic high-temperature hydrothermal alteration; the negative $\delta^{18}\text{O}$ values in the pre-metamorphic protolith were reequilibrated during eclogite facies metamorphism. Our results are consistent and comparable with the hydrothermal meteoric water alteration to the UHP eclogites and granitic gneisses in the Dabie-Sulu orogenic belt.

6. Conclusions

The Permian-age Group I eclogites formed from equivalents of the Panjal Traps and contain low- $\delta^{18}\text{O}$ igneous zircons preserved from

unusual, low- $\delta^{18}\text{O}$ mantle-derived magmas with hydrothermally altered subducted protoliths. The core domains of zircons in felsic gneisses also have lower $\delta^{18}\text{O}$ than the normal mantle-equilibrated value. After crystallization, these rocks were hydrothermally altered by heated meteoric water shifting $\delta^{18}\text{O}$ to negative values. Finally, during subduction of the Indian plate under Asia in the Eocene, $\delta^{18}\text{O}$ values in newly formed zircons were reequilibrated during UHP metamorphism in Group II eclogites and rim domains of zircons in felsic gneisses.

Supplementary data to this article can be found online at <https://doi.org/10.1016/j.gr.2017.12.004>.

Acknowledgements

We thank Noriko Kita and Jim Kern of the WiscSIMS Lab for help during SIMS analysis of $\delta^{18}\text{O}$. We also thank Emily Hung for help in zircon U–Pb age and Hf isotope analyses. We appreciate constructive reviews by two anonymous reviewers and suggestions by Journal Editor Alan Collins. This work was supported by the JSPS Research Fund (Kakenhi # 15K05316 and by the MOST project # 1050021585). The WiscSIMS Lab is supported by NSF (EAR-1355590) and the University of Wisconsin–Madison.

References

- Belousova, E.A., Kostitsyn, Y.A., Griffin, W.L., Begg, G.C., O'Reilly, S.Y., Pearson, N.J., 2010. The growth of the continental crust: constraints from zircon Hf-isotope data. *Lithos* 119, 457–466.
- Bindeman, I.N., Valley, J.W., 2001. Low- $\delta^{18}\text{O}$ rhyolites from Yellowstone: magmatic evolution based on analyses of zircons and individual phenocrysts. *Journal of Petrology* 42, 1491–1517.
- Bindeman, I.N., Fu, B., Kita, N., Valley, J.W., 2008. Origin and evolution of silicic magmatism at Yellowstone based on ion microprobe analysis of isotopically zoned zircons. *Journal of Petrology* 49, 163–193.
- Blum, T.B., Kitajima, K., Nakashima, D., Spicuzza, M.J., Strickland, A., Valley, J.W., 2016. Low- $\delta^{18}\text{O}$ magmas of the Lake Owyhee volcanic field, Oregon: implications for low- $\delta^{18}\text{O}$ magmas of the Snake River Plain - Yellowstone hotspot and other low- $\delta^{18}\text{O}$ large igneous provinces. *Contributions to Mineralogy and Petrology* 171:92. <https://doi.org/10.1007/s00410-016-1297-x>.
- Bowman, J.R., Moser, D.E., Valley, J.W., Wooden, J.L., Kita, N.T., Mazdab, F.K., 2011. Zircon U–Pb isotope $\delta^{18}\text{O}$ and trace element response to 80 m.y. of high temperature metamorphism in the lower crust: sluggish diffusion and new records of Archean craton formation. *American Journal of Science* 311, 719–727.
- Cartwright, I., Valley, J.W., 1991. Low- $\delta^{18}\text{O}$ Scourie dike magmas from the Lewisian Complex, northwestern Scotland. *Geology* 19, 578–581.
- Cartwright, I., Valley, J.W., 1992. Oxygen isotope geochemistry of the Scourian Complex, NW Scotland. *Journal of the Geological Society, London* 149, 115–126.
- Cawood, P.A., Johnson, M.R.W., Nemchin, A.A., 2007. Early Palaeozoic orogenesis along the Indian margin of Gondwana: tectonic response to Gondwana assembly. *Earth and Planetary Science Letters* 255, 70–84.
- Chen, Y.X., Zheng, Y.F., Chen, R.X., Zhang, S.B., Li, Q., Dai, M., Chen, L., 2011. Metamorphic growth and recrystallization of zircons in extremely ^{18}O -depleted rocks during eclogite-facies metamorphism: evidence from U–Pb ages, trace elements, and O–Hf isotopes. *Geochimica et Cosmochimica Acta* 75, 4877–4898.
- Compston, W., Williams, I.S., Meyer, C., 1984. U–Pb geochronology of zircons from lunar breccia 73217 using a sensitive high mass-resolution ion microprobe. *Journal of Geophysical Research* 89B, 525–534.
- Criss, R.E., Taylor, H.P., 1986. Meteoric-hydrothermal systems. In: Valley, J.W., Taylor Jr., H.P., O'Neil, J.R. (Eds.), *Stable Isotopes in High Temperature Geological Processes*. *Reviews in Mineralogy* 16, pp. 373–424.
- Curtis, C.G., Harris, C., Trumbull, R.B., Beer, C., Mudzanani, L., 2013. Oxygen isotope diversity in the anorogenic Koegel Fontein Complex of South Africa: a case for basement control and selective melting for the production of low $\delta^{18}\text{O}$ magmas. *Journal of Petrology* 54, 1259–1283.
- Davies, J.H.F.L., Stern, R.A., Heaman, L.M., Rojas, X., Walton, E.L., 2015. Resolving oxygen isotope disturbance in zircon: a case study from the low $\delta^{18}\text{O}$ Scourie dikes, NW Scotland. *American Mineralogist* 100, 1952–1966.
- Eiler, J.M., 2001. Oxygen isotope variations of basaltic lavas and upper mantle rocks. In: Valley, J.W., Cole, D.R. (Eds.), *Stable Isotope Geochemistry*. *Stable Isotope, Reviews in Mineralogy and Geochemistry* 43, pp. 319–364.
- Fu, B., Kita, N., Wilde, S.A., Liu, X., Cliff, J., Greig, A., 2013. Origin of the Tongbai-Dabie-Sulu Neoproterozoic low- $\delta^{18}\text{O}$ igneous province, east-central China. *Contributions in Mineralogy and Petrology* 165, pp. 641–662.
- Garlick, G.D., MacGregor, I.D., Vogel, D.E., 1971. Oxygen isotope ratios in eclogites from kimberlites. *Science* 172, 1025–1027.
- Gebauer, D., 1996. A P–T–t-path for an (ultra?) high-pressure ultramafic/mafic rock-association and its felsic country-rocks based on SHRIMP-dating of magmatic and metamorphic zircon domains. Example: Alpe Arami (Central Swiss Alps). In: Basu, A., Hart, S.R. (Eds.), *Earth Processes: Reading the Isotopic Code*. *American Geophysical Union*, pp. 309–328.

- Hartley, M.E., Thordarson, T., Fitton, J.G., EIMF, 2013. Oxygen isotopes in melt inclusions and glasses from the Askja volcanic system, North Iceland. *Geochimica et Cosmochimica Acta* 123, 55–73.
- He, Q., Zhang, S.-B., Zheng, Y.-F., 2016. High temperature glacial meltwater-rock reaction in the Neoproterozoic: evidence from zircon in-situ oxygen isotopes in granitic gneiss from the Sulu orogen. *Precambrian Research* 284, 1–13.
- Hoefs, J., 2015. *Stable Isotope Geochemistry*. 7th edition. Springer-Verlag, Berlin (389 pp.).
- Kaneko, Y., Katayama, I., Yamamoto, H., Misawa, K., Ishikawa, M., Rehman, H.U., Kausar, A.B., Shiraiishi, K., 2003. Timing of Himalayan ultrahigh-pressure metamorphism: sinking rate and subduction angle of the Indian continental crust beneath Asia. *Journal of Metamorphic Geology* 21, 589–599.
- Kita, N.T., Ushikubo, T., Fu, B., Valley, J.W., 2009. High precision SIMS oxygen isotope analysis and the effect of sample topography. *Chemical Geology* 264, 43–57.
- Kitajima, K., Ushikubo, T., Kita, N.T., Maruyama, S., Valley, J.W., 2012. Relative retention of trace element and oxygen isotope ratios in zircon from Archean rhyolite, Panorama Formation, North Pole Dome, Pilbara Craton, Western Australia. *Chemical Geology* 332–333, 102–115.
- Liati, A., Gebauer, D., 1999. Constraining the prograde and retrograde P–T–t path of Eocene HP rocks by SHRIMP dating different zircon domains: inferred rates of heating, burial, cooling and exhumation for central Rhodope, northern Greece. *Contributions to Mineralogy and Petrology* 135, 340–354.
- Liu, D., Ping Jian, P., Kröner, A., Xu, S., 2006. Dating of prograde metamorphic events deciphered from episodic zircon growth in rocks of the Dabie-Sulu UHP complex, China. *Earth and Planetary Science Letters* 250, 650–666.
- Miller, C., Thöni, M., Frank, W., Grasmann, B., Klötzli, U., Guntli, P., Dragantis, E., 2001. The early Paleozoic magmatic event in the northwest Himalaya, India: source, tectonic setting and age of emplacement. *Geological Magazine* 138, 237–251.
- Naeem, M., Burg, J.P., Ahmad, N., Chaudhry, M.N., Khalid, P., 2016. U–Pb zircon systematic of the Mansehra Granitic Complex: implications on the early Paleozoic orogenesis in NW Himalaya of Pakistan. *Geosciences Journal* 20, 427–447.
- O'Brien, P.J., Zotov, N., Law, R., Khan, M.A., Jan, M.Q., 2001. Coesite in Himalayan eclogite and implications for models of India-Asia collision. *Geology* 29, 435–438.
- Page, F.Z., Ushikubo, T., Kita, N.T., Riciputi, L.R., Valley, J.W., 2007. High-precision oxygen isotope analysis of picogram samples reveals 2 μm gradients and slow diffusion in zircon. *American Mineralogist* 92, 1772–1775.
- Peck, W.H., Valley, J.W., Graham, C.M., 2003. Slow oxygen diffusion rates in igneous zircons from metamorphic rocks. *American Mineralogist* 88, 1003–1014.
- Rehman, H.U., Yamamoto, H., Kaneko, Y., Kausar, A.B., Murata, M., Ozawa, H., 2007. Thermobaric structure of the Himalayan metamorphic belt in Kaghan Valley, Pakistan. *Journal of Asian Earth Sciences* 29, 390–406.
- Rehman, H.U., Kobayashi, K., Tsujimori, T., Ota, T., Yamamoto, H., Nakamura, E., Kaneko, Y., Khan, T., Terabayashi, M., Yoshida, K., Hirajima, T., 2013a. Ion microprobe U–Th–Pb geochronology and study of micro-inclusions in zircon from the Himalayan high and ultrahigh-pressure eclogites, Kaghan Valley of Pakistan. *Journal of Asian Earth Sciences* 63, 179–196.
- Rehman, H.U., Yamamoto, H., SHIN, K., 2013b. Metamorphic P–T evolution of high-pressure eclogites from garnet growth and reaction textures: insights from the Kaghan Valley transect, northern Pakistan. *Island Arc* 22, 4–24.
- Rehman, H.U., Tanaka, R., O'Brien, P.J., Kobayashi, K., Tsujimori, T., Nakamura, E., Yamamoto, H., Khan, T., Kaneko, Y., 2014. Oxygen isotopes in Indian Plate eclogites (Kaghan Valley, Pakistan): negative $\delta^{18}\text{O}$ values from a high latitude protolith reset by Himalayan metamorphism. *Lithos* 208–209, 471–483.
- Rehman, H.U., Lee, H.Y., Chung, S.L., Khan, T., O'Brien, P.J., Yamamoto, H., 2016. Source and mode of the Permian Panjal Trap magmatism: evidence from zircon U–Pb and Hf isotopes and trace element data from the Himalayan ultrahigh-pressure rocks. *Lithos* 260, 286–299.
- Rehman, H.U., Jan, M.Q., Khan, T., Yamamoto, H., Kaneko, Y., 2017. Varieties of the Himalayan eclogites: a pictorial review of textural and petrological features. *Island Arc* 26, 1–14 (e12209).
- Rumble, D., Giorgis, D., Ireland, T., Zhang, Z., Xu, H., Yui, T.F., Yang, J., Xu, Z., 2002. Low $\delta^{18}\text{O}$ zircons, U–Pb dating, and the age of the Qinglongshan oxygen and hydrogen isotope anomaly near Donghai in Jiangsu Province, China. *Geochimica et Cosmochimica Acta* 66, 2299–2306.
- Schulze, D.J., Harte, B., EIMF, Page, F.Z., Valley, J.W., Channer, D.M.D.R., Jaques, A.L., 2013. Anticorrelation of isotope signatures of carbon in eclogitic diamonds and oxygen in their silicate mineral inclusions requires subducted source material for eclogitic diamonds. *Geology* 41, 455–458.
- Valley, J.W., 1986. Stable isotope geochemistry of metamorphic rocks. In: Valley, J.W., Taylor Jr., H.P., O'Neil, J.R. (Eds.), *Stable Isotopes in High Temperature Geological Processes*. Reviews in Mineralogy 16, pp. 445–489.
- Valley, J.W., 2003. Oxygen isotopes in zircon. In: Hancher, J.M., Hoskin, W.O. (Eds.), *Reviews in Mineralogy and Geochemistry*. 53, pp. 343–385.
- Valley, J.W., Kita, N.T., 2009. In situ oxygen isotope geochemistry by ion microprobe. *Mineralogical Association of Canada Short Course*. 41, pp. 19–63.
- Valley, J.W., Chiarenzelli, J.R., McLelland, J.M., 1994. Oxygen isotope chemistry of zircon. *Earth and Planetary Science Letters* 126, 187–206.
- Valley, J.W., Bindeman, I.N., Peck, W.H., 2003. Empirical calibration of oxygen isotope fractionation in zircon. *Geochimica et Cosmochimica Acta* 67, 3257–3266.
- Valley, J.W., Lackey, J.S., Cavosie, A.J., Clechenko, C.C., Spicuzza, M.J., Basei, M.A.S., Bindeman, I.N., Ferreira, V.P., Sial, A.N., King, E.M., Peck, W.H., Sinha, A.K., Wei, C.S., 2005. 4.4 billion years of crustal maturation: oxygen isotope ratios of magmatic zircon. *Contributions to Mineralogy and Petrology* 150, 561–580.
- Valley, J.W., Reinhard, D.A., Cavosie, A.J., Ushikubo, T., Lawrence, D.F., Larson, D.J., Kelly, T.F., Snoeyenbos, D., Strickland, A., 2015. Nano- and micro-geochronology in hadean and archean zircons by atom-probe tomography and SIMS: new tools for old minerals. *American Mineralogist* 100:1355–1377. <https://doi.org/10.2138/am-2014-5134>.
- Wan, Y.S., Zhang, J.H., Williams, I.S., Liu, D.Y., Dong, C.Y., Fan, R.L., Shi, Y.R., Ma, M.Z., 2013. Extreme zircon O isotopic compositions from 3.8 to 2.5 Ga magmatic rocks from the Anshan area, North China Craton. *Chemical Geology* 352, 108–124.
- Wang, X.C., Li, Z.X., Li, X.H., Li, Q.L., Tang, G.Q., Zhang, Q.R., Liu, Y., 2011. Nonglacial origin for low- $\delta^{18}\text{O}$ Neoproterozoic magmas in the South China Block: evidence from new in-situ oxygen isotope analysis using SIMS. *Geology* 39, 735–738.
- Wang, X.-L., Coble, M.A., Valley, J.W., Shu, X.-J., Kitajima, K., Spicuzza, M.J., Sun, T., 2014. Influence of radiation damage on late Jurassic zircon from southern China: evidence from in situ measurement of oxygen isotopes, laser Raman, U–Pb ages, and trace elements. *Chemical Geology* 389, 122–136.
- Wasserburg, G.J., Papanastassiou, D.A., Nienow, E.V., Baumann, C.A., 1969. A programmable magnetic field mass spectrometer with on-line data processing. *The Review of Scientific Instruments* 40, 288–295.
- Watson, E.B., Cherniak, D.J., 1997. Oxygen diffusion in zircon. *Earth and Planetary Science Letters* 148, 527–544.
- Wei, C.S., Zheng, Y.F., Zhao, Z.F., Valley, J.W., 2002. Oxygen and neodymium isotope evidence for recycling of juvenile crust in northeast China. *Geology* 30, 375–378.
- Wei, C.S., Zhao, Z.F., Spicuzza, M.J., 2008. Zircon oxygen isotopic constraint on the sources of late Mesozoic A-type granites in eastern China. *Chemical Geology* 250, 1–15.
- Yui, T.F., Rumble, D., Lo, C.H., 1995. Unusually low $\delta^{18}\text{O}$ ultra-high-pressure metamorphic rocks from the Sulu Terrain, eastern China. *Geochimica et Cosmochimica Acta* 59, 2859–2864.
- Zhao, Z.F., Zheng, Y.F., 2003. Calculation of oxygen isotope fractionation in magmatic rocks. *Chemical Geology* 193, 59–80.
- Zheng, Y.F., Fu, B., 1998. Estimation of oxygen diffusivity from anion porosity in minerals. *Geochemical Journal* 32, 71–89.
- Zheng, Y.F., Fu, B., Li, Y., Xiao, Y., Li, S., 1998. Oxygen and hydrogen isotope geochemistry of ultrahigh-pressure eclogites from the Dabie Mountains and the Sulu terrane. *Earth and Planetary Science Letters* 155, 113–129.
- Zheng, Y.F., Fu, B., Gong, B., Li, L., 2003. Stable isotope geochemistry of ultrahigh pressure metamorphic rocks from the Dabie-Sulu orogen in China: implications for geodynamics and fluid regime. *Earth-Science Reviews* 62, 105–161.
- Zheng, Y.F., Wu, Y.-B., Chen, F.K., Gong, B., Li, L., Zhao, Z.F., 2004. Zircon U–Pb and oxygen isotope evidence for a large-scale ^{18}O depletion event in igneous rocks during the Neoproterozoic. *Geochimica et Cosmochimica Acta* 68, 4145–4165.
- Zheng, Y.F., Wu, Y.-B., Gong, B., Chen, R.-X., Tang, J., Zhao, Z.F., 2007. Tectonic driving of Neoproterozoic glaciations: evidence from extreme oxygen isotope signature of meteoric water in granite. *Earth and Planetary Science Letters* 256, 196–210.
- Zheng, Y.F., Gong, B., Zhao, Z.F., Wu, Y.B., Chen, F.K., 2008. Zircon U–Pb age and O isotope evidence for Neoproterozoic low- ^{18}O magmatism during supercontinental rifting in South China: implications for snowball Earth event. *American Journal of Science* 308, 484–516.
- Zhu, D.C., Zhao, Z.D., Niu, Y., Dilek, Y., Wang, Q., Ji, W.H., Dong, G.C., Sui, Q.L., Liu, Y.S., Yuan, H.L., Mo, X.X., 2012. Cambrian bimodal volcanism in the Lhasa Terrane, southern Tibet: record of an early Paleozoic Andean-type magmatic arc in the Australian proto-Tethyan margin. *Chemical Geology* 328, 290–308.